atmosphere

MDPI

Article

Characteristics of BVOCs from Fragrant Flowering Trees and Their Emission Along Urban Roadsides in Shanghai, China

Xi Wang [1,2,†], Yin Wu [1,†], Yanting Zhang [3], Ruiqing Yang [3], Mengwei Fang [1,2], Benyao Wang [3], Yali Zhang [1,*] and Meixian Wang [2,*]

[1] Shanghai Academy of Agricultural Sciences, Shanghai 201403, China; wx2001@bjfu.edu.cn (X.W.); wyshnky@saas.sh.cn (Y.W.); fangmengwei@bjfu.edu.cn (M.F.)
[2] School of Landscape Architecture, Beijing Forestry University, Beijing 100083, China
[3] Shanghai Municipal Landscape Management and Guidance Station, Shanghai Engineering Research Center of Urban Trees Ecological Application, Shanghai 200020, China; hilary.kk@hotmail.com (Y.Z.); zdzyrq@163.com (R.Y.); wangbenyao@163.com (B.W.)
* Correspondence: zhangyl@saas.sh.cn (Y.Z.); wangmx@bjfu.edu.cn (M.W.)
† These authors contributed equally to this work.

Abstract

Flowering street trees provide ecological services and health benefits to humans. In this study, three commonly used flowering street trees, *Paulownia tomentosa* (Thunb.) Steud., *Melia azedarach* L., and *Magnolia grandiflora* L., were selected for analysis of floral volatiles during different flowering stages along roadsides in Shanghai, China. Headspace sampling solid-phase microextraction (HS–SPME) coupled with gas chromatography–mass spectrometry (GC–MS) was used to identify volatiles from different floral samples. Simultaneously, selected-ion flow-tube mass spectrometry (SIFT–MS) was employed to detect biogenic volatile organic compounds (BVOCs) in roadside air samples. The results indicated that (1) *P. tomentosa* volatiles consisted predominantly of alcohols and phenolic ethers, *M. azedarach* volatiles consisted primarily of alcohols and aldehydes, and *M. grandiflora* volatiles consisted mainly of terpenes. (2) Air samples from *P. tomentosa and M. azedarach* were dominated by alcohols, whereas air samples from *M. grandiflora* were dominated by terpenes and aldehydes. The ozone formation potential (***OFP***) of some VOCs fluctuated throughout the flowering period. (3) Antibacterial and antioxidant volatiles released from the flowers of all species, such as eugenol, have demonstrated health-promoting effects in essential oils. The results of this study provide a foundation for optimizing the selection and planting of flowering street trees in urban roadside areas that will enhance ecological services and public health benefits.

Keywords: flowering street trees; flowering period; biogenic volatile organic compounds; ozone formation potential

Check for updates

Academic Editor: Iustinian Gabriel Bejan

Received: 7 January 2026
Revised: 5 February 2026
Accepted: 7 February 2026
Published: 8 February 2026

Copyright: © 2026 by the authors. Licensee MDPI, Basel, Switzerland. This article is an open access article distributed under the terms and conditions of the Creative Commons Attribution (CC BY) license.

1. Introduction

Biogenic volatile organic compounds (BVOCs) are secondary metabolites emitted by plants. Among identified floral volatiles, terpenoids predominate, followed by aliphatic compounds, aromatic compounds, oxygen-containing compounds, and sulfur-containing compounds. BVOCs are typically categorized into three groups: terpenes, phenyl compounds, and fatty acid derivatives [1,2]. BVOCs are important for human health and well-being because they alleviate human stress, exhibit anti-inflammatory and antibacterial properties, remove ozone and particulate matter, and provide raw materials for

perfumes and pharmaceuticals [3–5]. BVOCs play an important role in research and practical applications.

Current research on floral volatile organic compounds primarily encompasses beneficial volatiles and their functions, as well as the emission mechanisms and temporal dynamics of BVOCs. Previous analyses of volatiles and their emission patterns have demonstrated variation in the type and content of BVOCs produced by plants from different origins [6], at different flowering stages [7], and from different floral organs [8,9]. Plant volatiles are predominantly collected using steam distillation and headspace sampling solid-phase microextraction (HS–SPME) [10]. The primary analytical methods for identifying plant volatiles include gas chromatography–mass spectrometry (GC–MS) [11], gas chromatography–olfactometry mass spectrometry (GC–O–MS) [12], and electronic nose technology [13]. Some researchers have employed multiple methods concurrently [14]. Overall, HS–SPME is currently the most widely used method for collecting and analyzing volatiles from living plants, and GC–MS is the most common method for identifying plant volatiles and enabling both qualitative and quantitative analysis of all or specific compounds in a sample.

The emission characteristics of BVOCs and their impact on air quality represent another field of research [15,16]. BVOCs react with hydroxyl radicals (OH) in the atmosphere to form peroxy radicals (RO_2). These peroxy radicals oxidize NO into NO_2, which undergoes photolysis under ultraviolet radiation to produce oxygen atoms (O). The oxygen atoms then combine with oxygen molecules (O_2) to ultimately form ozone (O_3) [17], which is one of the most harmful pollutants in the troposphere [18,19]. NO_x continuously undergoes consumption and regeneration throughout the cycle, acting as a catalyst. Meanwhile, BVOCs possess high chemical reactivity, effectively driving the radical cycle, and their contribution to O_3 formation cannot be overlooked. Numerous researchers have evaluated the impact of BVOCs on air quality based on precursor VOC concentrations, OH reaction rate constants, and species-specific maximum increment reactivity coefficients (MIR) [20–22]. This method explains the role of different VOCs in O_3 formation without considering NO_x concentrations. Furthermore, studies on VOC/NO_x sensitivity in O_3 formation have been conducted [23–26]. These studies employed various models, including the empirical kinetic modeling approach (EKMA), the observation-based model (OBM), an O_3 isopleth mapping software package (research edition) (OZIPR), and the weather research and forecasting atmospheric chemistry model (WRF-Chem), to conduct VOC/NO_x sensitivity analyses based on O_3 isopleth maps, which in turn revealed the complex interactions among NO_x, VOCs, and O_3.

Some studies have shown that substantial volatile emissions from plants may significantly impact air quality and human health [27–29]. Previous research has focused primarily on the volatiles of plants themselves and the impact of volatiles on air quality in forests or urban parks [30]. Urban roadside green belts are situated alongside traffic lanes, which produce high NO_x emissions and serve as vital daily passageways. As demands by citizens for relaxation in natural settings have increased, flowering trees along roadside have gained attention for their unique and diverse aesthetic and scientific value; in addition to their ornamental value, roadside trees may provide health benefits. In recent years, roadside plantings in Shanghai have been prioritized to enhance urban streets with color and fragrance. However, few studies have assessed the BVOCs produced by these plants or their effects on the environment and human health. Identifying the volatiles emitted by these flowering trees may have significant implications for the urban ecological environment and public well-being.

Paulownia tomentosa (Thunb.) Steud., *Melia azedarach* L., and *Magnolia grandiflora* L., which are characterized by high application frequency, strong adaptability, and pronounced

floral fragrance in Shanghai, were selected for this study. Current research on these street trees primarily focuses on extracting floral essential oils for component analysis. For instance, soxhlet extraction, steam distillation coupled with GC-MS, was used to isolate and analyze lipid-soluble components from *P. tomentosa* flowers [31]. A total of 63 volatile compounds were identified in the essential oil of *M. azedarach* flowers using GC-MS, which demonstrated the oil's inhibitory effect on certain bacteria [32]. A total of 80 volatile compounds were identified in the essential oil of *M. grandiflora* flowers using GC-MS. However, studies on the BVOCs of fresh flowers and their effects on human health and air quality remain scarce [33].

Thus, the objectives of the present study are as follows: (1) To detect and analyze dynamic changes in flower BVOC emissions from different fresh samples, (2) To investigate the dominant volatiles released by plants into roadside air and evaluate their ***OFP*** (ozone formation potential), and (3) to provide a reference for the application and planning of sustainable urban ecosystems in Shanghai and similar high-density cities in the future, so as to achieve synergistic benefits in urban greening that will enhance landscape aesthetics, regulate ecosystems, and promote public health.

2. Materials and Methods

2.1. Analysis of Floral Volatiles

2.1.1. Materials, Instruments, and Reagents

Three species of fragrant flowering street tree were selected. Fresh samples of *P. tomentosa* were collected from Zichang Road in the Putuo District, samples of *M. azedarach* were collected from Yangcheng Road in the Jing'an District (between Yuanping Road and Hutaizhi Road), and samples of *M. grandiflora* were collected from Ronghua West Road in the Changning District (between Shuicheng South Road and Shuicheng South Road). All of the samples were collected during the full-blooming period of the trees, and floral organs were collected at the DL (bud stage), CH (initial bloom stage), and SH (bloom stage) developmental stages. During each flowering period, plants with consistent growth and that were free of pests or diseases were selected. For *P. tomentosa* and *M. grandiflora*, 3–5 fresh flowers from each flowering stage were collected. For *M. azedarach*, 15–30 fresh flowers were collected. All flowers were chopped into uniform pieces, thoroughly mixed, and 1 g of each flower was accurately weighed from each flowering period for analysis (Figure 1).

A 1 g sample was transferred into a 20 mL headspace vial along with 10 μL of ethyl decanoate (0.865 μg/μL, purity: >99%, M23GB142678, Yuanye Biotechnology Co., Ltd., Shanghai, China) as an internal standard and 5 mL saturated NaCl solution (purity: 99.5%, JS322469, Yuanye Biotechnology Co., Ltd., Shanghai, China). The headspace vial was promptly sealed and equilibrated at room temperature for 1 h before HS–SPME and GC–MS analysis. Each sample was replicated 3 times.

Analyses were performed at the Shanghai Academy of Agricultural Sciences (Shanghai, China) using an Agilent 7890A-5975C GC–MS system (Agilent Technologies, Inc., Santa Clara, CA, USA) with an Agilent 122-7062UI DB-WAX UI column (60 m × 250 μm × 0.25 μm) and a DVB/CAR/PDMS 50/30 μm extraction head (Supelco, Inc., Bellefonte, PA, USA). Extraction was performed with an agitator oven temperature of 50 °C, agitation at 250 times/min, and an incubation time of 10 min. The GC injector temperature and split ratio were set at 220 °C. The temperature program for GC started at 40 °C for 3 min, then increased at a rate of 3 °C/min to 70 °C, increasing again at a rate of 5 °C/min to 180 °C, and then again at a rate of 10 °C/min to 220 °C for a hold time of 7 min. Ultrahigh purity helium was used as a carrier gas with a flow rate at 1.00 mL/min and the ion source temperature and interface temperature for MS were 250 °C. Detection

was performed using electron ionization at 70 eV with a scan range of 30–300 m/z and an initial scan time of 5 min.



Figure 1. Fresh samples collected from fragrant flowering street trees. (**A**,**B**,**C**) represent *P. tomentosa*, *M. azedarach*, and *M. grandiflora* respectively; DL (bud stage), CH (initial bloom stage), and SH (bloom stage).

2.1.2. Data Processing

Each sample underwent triplicate parallel measurements, and the results are expressed as the mean ± the standard deviation. BVOCs were qualitatively identified using the automatic deconvolution system associated with the GC–MS workstation, the NIST05a.L spectral library, and compound retention indices. The absolute concentration of BVOCs relative to the internal standard was calculated by comparing the chromatographic peak area of the target volatile with that of the internal standard, based on the internal standard content.

$$C_x = M \times \frac{A_i}{m} \times A_0 \quad (1)$$

where C_x is the absolute concentration of the analyte (μg/g), M is the mass of the internal standard (μg), m is the sample weight (g), A_i is the peak area of the analyte, and A_0 is the peak area of the internal standard.

2.2. Air Sampling and Methods of Analysis for Fragrant Flowering Street Trees

2.2.1. Sampling Method

Open-air sampling was conducted using a gas collection bag. Sampling occurred on a clear, windless day. During sampling, flowering processes of different trees along the same road did not progress entirely synchronously due to factors such as road microclimate, thus samples can simultaneously reflect BVOCs released into the air during DL, CH, SH. This facilitates the selection of key target compounds from air samples for further analysis compared with BVOCs emitted by floral parts across 3 periods. Five sampling points were selected along the road where subjective floral scent was the most concentrated. Three replicates were established for each points. Prior to sampling, the collection bags

underwent 3 cycles of vacuuming and inflation to purge residual air, followed by cyclic sampling. Handheld clean silicone tubing was used for sampling beneath trees at human breathing height (approximately 1.5 m above ground). At each sampling point, air around the tree trunk was dynamically collected in 4 mutually perpendicular directions centered on the trunk with a radius of 1 m. After sampling, the sampler was allowed to rest for 10 min.

2.2.2. Analytical Method

The following parameters were used for analysis: 40 cm^3/min sample gas flow, 156 cm^3/min helium carrier gas flow, 50 V flow tube voltage, 120 °C flow tube temperature, and 105 °C sample plate and sampling tube heater temperature. A SYFT Voice200 ULTRA advanced SIFT–MS (Syft Technologies, Christchurch, New Zealand) was used to measure volatile compound concentrations in roadside air near 3 species of fragrant flowering street trees. All of the detected floral volatile compounds were matched against compound information (collision constants, reaction rate constants, reaction rates, and other factors) from the Syft compound library. Volatiles with relevant parameters in the library were selected as targets for analysis. Each replicate was analyzed 5 times.

2.2.3. Health Risk Assessment Indicators

High concentrations of ground-level ozone pose multiple health hazards to humans. The ozone formation potential (***OFP***) measures the potential capacity of VOCs to undergo photochemical reactions with NO_x in sunlight, thereby generating ground-level ozone. The ***OFP*** indirectly supports public health risk management by aiding the regulation and control of ozone precursors such as VOCs. It is calculated according to the following formula:

$$\boldsymbol{OFP} = \sum_{\boldsymbol{i}} \boldsymbol{C_i} \times \boldsymbol{MIR_i} \quad (2)$$

where $\boldsymbol{C_i}$ ($\mu g/m^3$) represents the absolute concentration of each VOC component in roadside air (VOC), derived from the sample mean, and ***MIR*** ($gVOC/gO_3$) is the maximum increment response coefficient referring to the research by Cater [22].

2.2.4. Data Analysis Methods

Data of BVOCs is exported by Agilent 7890A-5975C GC–MS system. Air sample data were exported from SYFT Voice200 ULTRA advanced SIFT–MS. Excel 2019 and Origin 2025 Pro were used to analysis and draw all figures.

3. Results

3.1. BVOCs from P. tomentosa Flowers and Their Emissions into Roadside Air

3.1.1. Analysis of Volatile Types and Absolute Concentrations

A total of 45 volatiles from *P. tomentosa* flowers were identified and annotated across samples from the DL, CH, and SH, and volatiles were categorized into 9 groups including alcohols, phenols, ethers, aldehydes, terpenes, ketones, alkanes, esters, and others. As shown in Figure 2, the absolute concentration of alcohols accounted for the highest proportion among all components during each flowering stage, representing 81.46%, 67.95%, and 31.34% during DL, CH, and SH respectively. Alcohols such as 1-octen-3-ol and benzyl alcohol were the most abundant type of volatile, particularly during DL and CH (Appendix A Table A1). The absolute concentration proportion of phenols, ethers, and terpenes gradually increased as the flowers bloomed, and those of other volatiles showed fluctuating trends. However, they have never exceeded the absolute percentage of alcohol concentration.

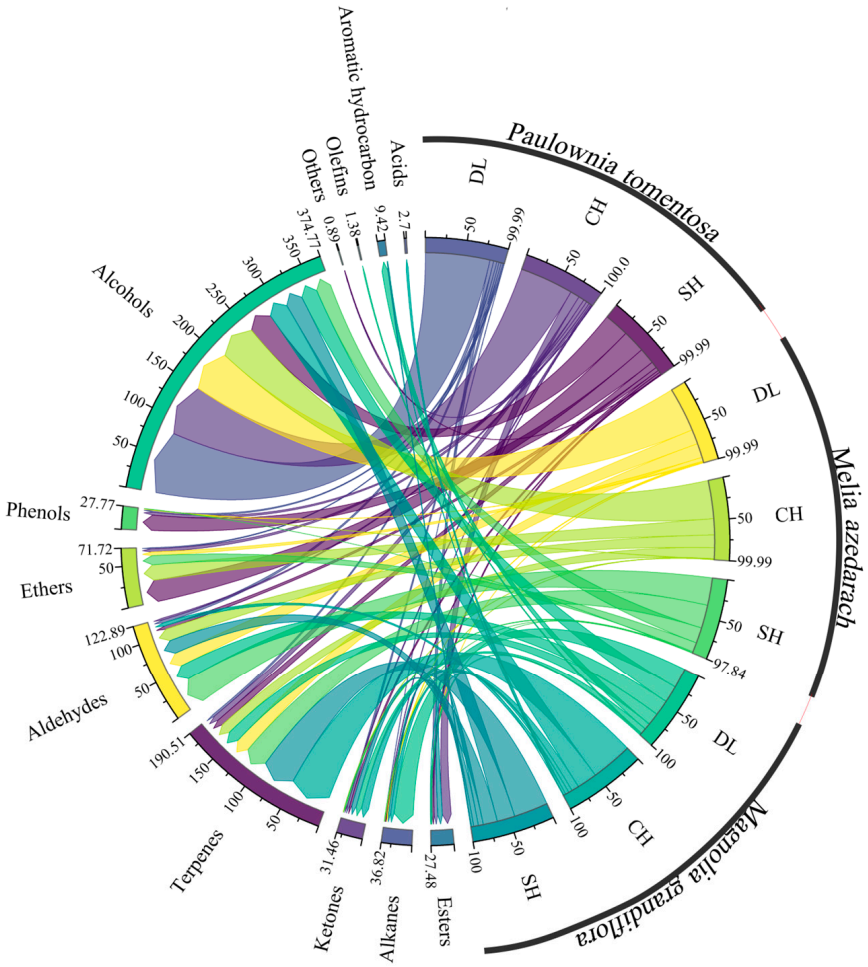


Figure 2. BVOC species and concentration proportions released by three street trees during DL, CH, and SH. Chord diagram width indicates the proportion contribution of each compound class to a given species and flowering stage.

A Venn diagram (Figure 3) illustrates that *P. tomentosa* shared 13 common volatiles across different flowering stages. Two unique compounds appeared during DL, four unique compounds appeared during CH, and eleven unique compounds appeared during SH. Among the common volatiles, absolute concentrations of 7 volatiles, including 1,2,4-trimethoxybenzene, benzyl alcohol, benzaldehyde, eugenol, anethol, methyl eugenol, and isoeugenol methyl ether, gradually increased over the course of blooming, while 1-octen-3-ol gradually decreased. The remaining five volatiles showed no obvious trend. Some compounds occurred during two flowering stages: 6,10-dimethylenonadecan-5,9-dien-2-ol, salicylaldehyde, an ocimene mixture of isomers, (E)-β-aacadienol, and β-caryophyllene increased in absolute concentration during SH compared with CH, while 2-methoxy-4-methylphenol, dodecane, and n-hexanol exhibited decreases, albeit relatively minor ones. Phenethyl alcohol, phenol, geranylacetone, and benzoic acid benzyl ester increased in absolute concentration during CH relative to DL. Phellandrene and nerolidol were identified during DL and SH, and their absolute concentrations were significantly higher during SH than during DL.

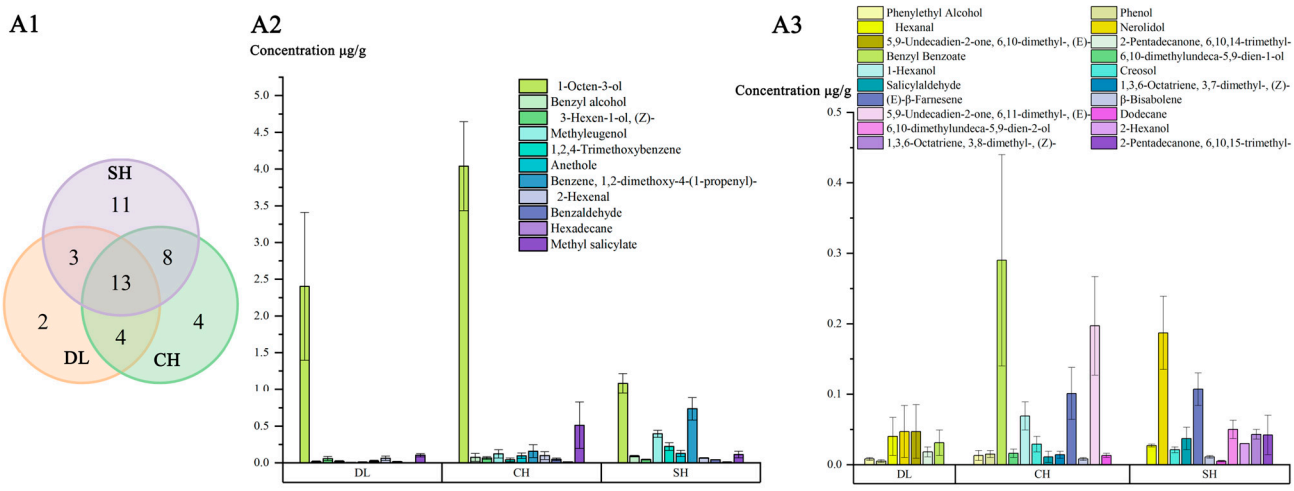


Figure 3. Types and absolute concentration of BVOCs at different flowering stages of *P. tomentosa*. The numbers in the (**A1**) overlapping sections represent the types of components common to different periods, while the non-overlapping sections indicate the types of components unique to that period. In (**A2**) we see the absolute concentration of common volatiles and (**A3**) shows the absolute concentration of unique volatiles at different flowering stages.

3.1.2. Release of VOCs into Roadside Air

Considering that different stages of flowering overlap during the blossoming of urban roadside trees, BVOCs identified from 3 flowering stages were used as baseline data in this study. Twelve target volatiles were selected for emission analysis for *P. tomentosa*, combined with compound information in the Syft Library, and the concentrations of volatiles in the air are shown in Figure 4.

Twelve target volatiles were detected along the road where *P. tomentosa* were planted. The average concentrations of the 12 target volatiles ranged from 11.668–333.07 μg/m^3, 1-octen-3-ol and anethole were detected at all sampling points. The concentration of 1-octen-3-ol ranged from 187.08–545.77 μg/m^3, while that for anethole ranged from 14.02–55.09 μg/m^3. Benzyl alcohol, eugenol, and methyl salicylate were detected at only one sampling site, and eugenol exhibited a higher concentration than the other two compounds. Overall, alcohols accounted for 73.00% of all the target volatiles from roadside air near *P. tomentosa*.

Five key VOCs were screened to calculate their ***OFP***, and Carter's MIR for specific VOCs was employed. The total ***OFP*** initially increased and then decreased (Table 1). ***OFP*** of VOCs increased from DL (0.101 μg/m^3) to peak during CH (0.626 μg/m^3), representing a high-risk period for ozone formation, and then decreased to 0.581 μg/m^3. Emission patterns varied significantly among different compounds. For example, benzyl alcohol was continuously emitted throughout blooming, 1-hexanol, phenol, and dodecane exhibited relatively stable emission, and 4-Methylanisole was emitted only during SH. Among these compounds, benzyl alcohol appeared as a key contributor to ozone formation due to its high MIR value, continuously increasing ***OFP***, and significant contribution ratio. The contributions of other compounds to ozone formation fluctuated or decreased during different flowering stages, which demonstrated that the effects of different compounds on the environment were varied as the flowers bloomed.

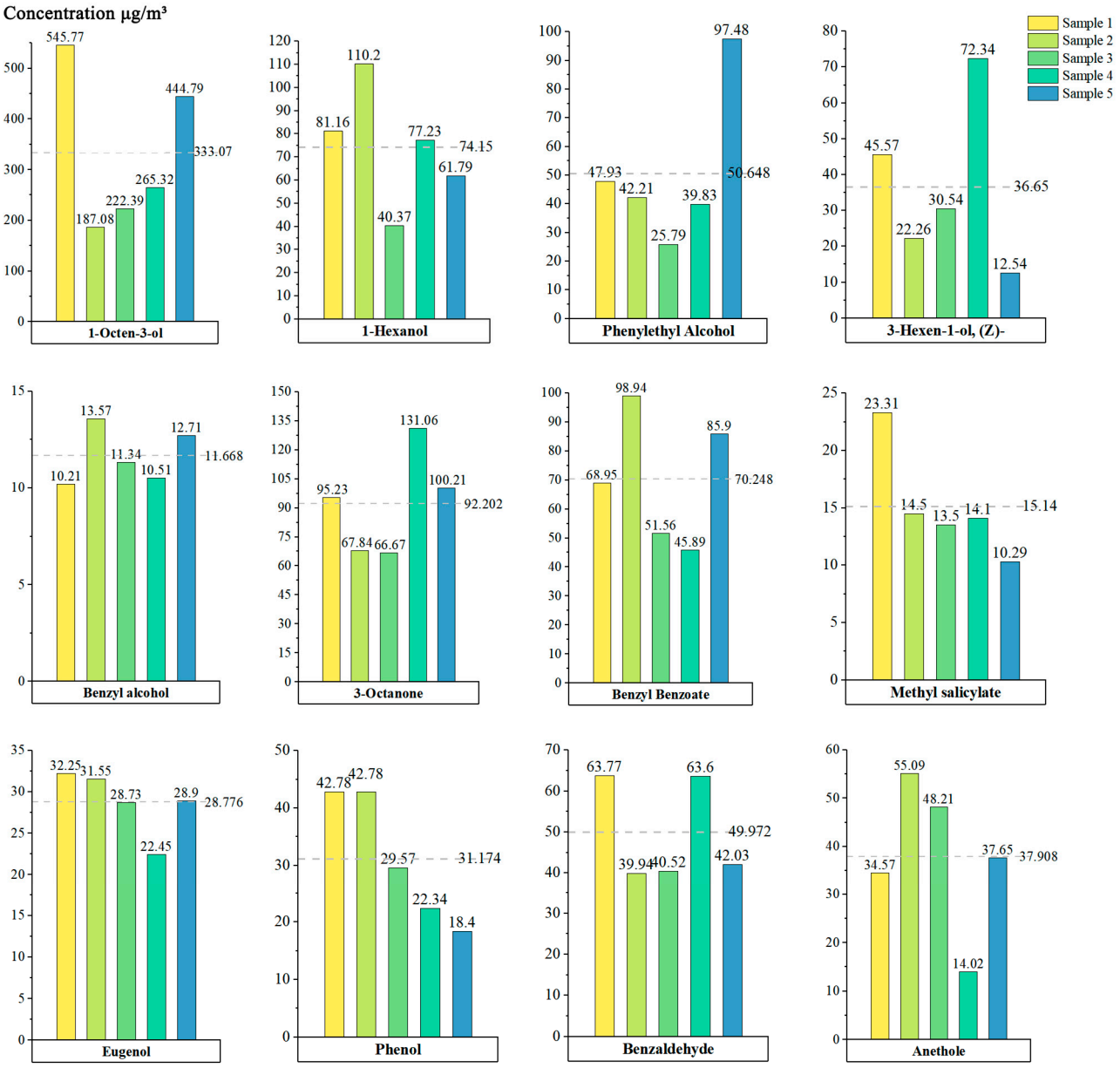


Figure 4. Twelve target VOCs in roadside air with *P. tomentosa*. The figure displays the average absolute concentrations of VOCs in the five sampling points, with dashed lines representing the average values.

Table 1. *OFP* of VOCs from *P. tomentosa* road at different flowering stages.

VOCs	MIR	*OFP* (μg/m^3)			Contribution Ratio to Ozone Generation (%)		
		DL	CH	SH	DL	CH	SH
Benzyl alcohol	5.11	0.087	0.383	0.470	86.139	61.182	80.895
1-Hexanol	2.69	-	0.186	0.081	-	29.712	13.941
Phenol	2.76	0.014	0.041	-	13.861	6.550	
4-Methylanisole	2.36	-	-	0.024	-		4.131
Dodecane	1.25	-	0.016	0.006	-	2.556	1.033
Total	-	0.101	0.626	0.581	100	100	100

3.2. BVOCs from M. azedarach Flowers and Their Release into Roadside Air

3.2.1. Analysis of Volatile Types and Absolute Concentrations

A total of 34 volatiles from *M. azedarach* were identified and annotated across samples from DL, CH, and SH, and volatiles were categorized into nine groups, including phenols, ethers, esters, and alkanes. As shown in Figure 2, the absolute concentration of alcohols accounted for the highest proportion among all components, respectively accounting for 56.23% and 48.30% during the DL and CH, while during the SH, the absolute concentration proportion of terpenes became predominant, accounting for 34.86%. As flowers bloomed, the absolute concentration proportion of alcohol, alkane, and phenol in the samples gradually decreased. Alcohols decreased from 56.23% (DL) to 48.30% (CH) to 19.69% (SH), alkane decreased from 1.20% (DL) to 0.59% (CH) to 0.11% (SH), and phenol decreased from 0.63% (DL) to 0.31% (CH) to 0.18% (SH). According to Appendix A Table A2, ethyl alcohol had the highest concentration during CH, while the concentration of phenylethyl alcohol, benzaldehyde, benzene, 1,4-dimethoxy-, and phenol increased as the flowers bloomed. Conversely, 3-Hexen-1-ol, (Z)-, and nonanal gradually decreased.

Ten volatiles were common across all of the flowering stages of *M. azedarach*. Three unique compounds appeared during DL, two unique compounds appeared during CH, and ten unique compounds appeared during SH (Figure 5). Among the common volatiles, the absolute concentrations of phenethyl alcohol, benzaldehyde, p-dimethylbenzene, and phenol gradually increased as the flowers bloomed, while that of linalool and nonanal gradually decreased. The remaining four volatiles fluctuated. Nine volatiles were shared during the CH and SH stages: n-hexanol, 3-hexanol, and zingiberene decreased in absolute concentration as the flowers bloomed, while the other six volatiles increased. Among these, benzyl alcohol, (E)-β-farnesene, β-bisabolene, and geranylacetone increased significantly.

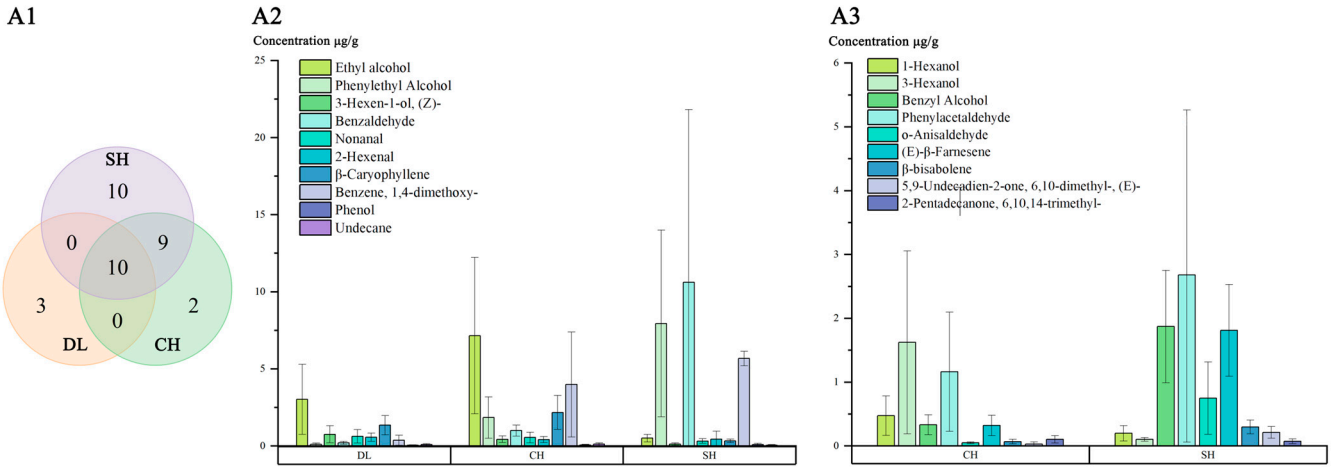


Figure 5. Types and absolute concentrations of BVOCs at different flowering stages of *M. azedarach*. The numbers in the (**A1**) overlapping sections represent the types of components common to different periods, while the non-overlapping sections indicate the types of components unique to that period. In (**A2**) we see the absolute concentration of common volatiles and (**A3**) shows the absolute concentration of unique volatiles at different flowering stages.

3.2.2. Release of VOCs into Roadside Air

Seven target volatiles were detected at sampling points along the roadside. Average concentrations ranged from 6.01 to 50.64 μg/m^3, but average concentrations of the same compound varied across different sampling points. Overall, alcohols constituted the highest proportion of volatiles in the roadside air, accounting for 64.77%, and phenethyl alcohol exhibited the highest concentration (Figure 6).

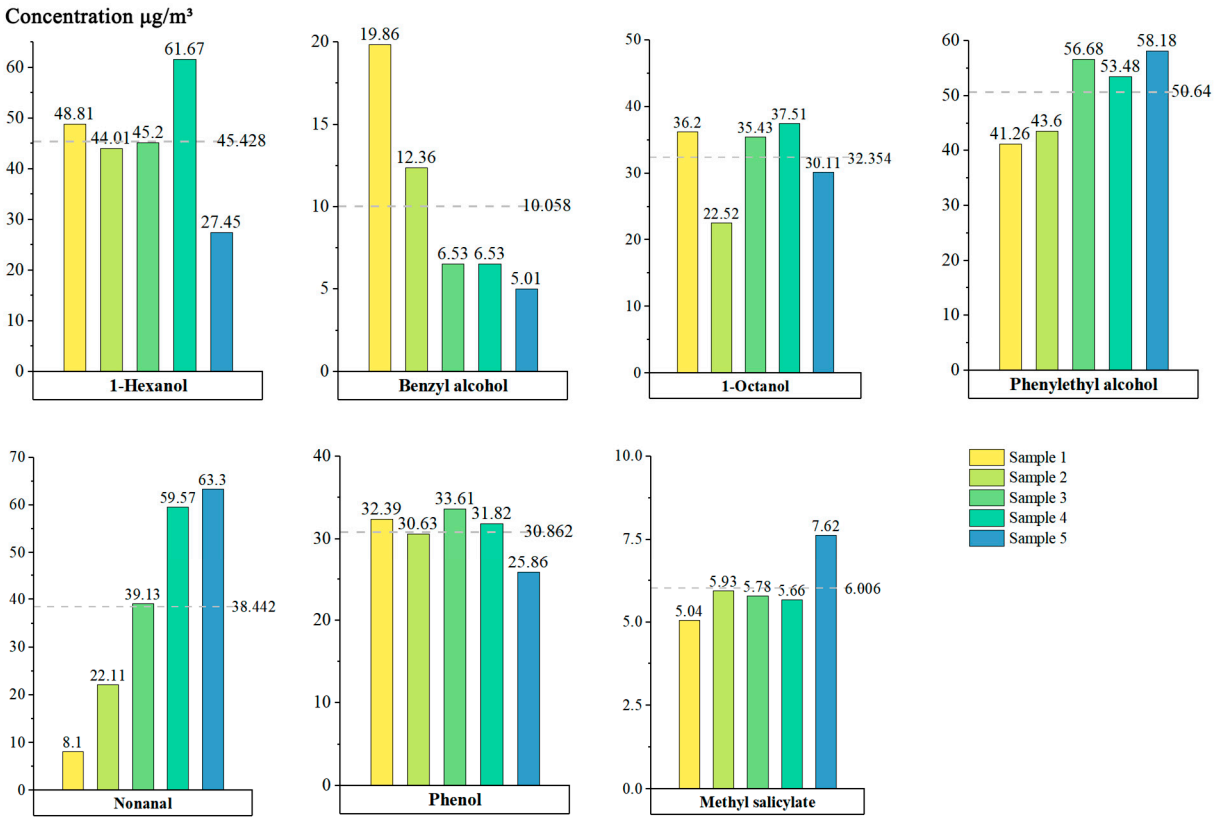


Figure 6. Seven target VOCs in roadside air with *M. azedarach*. The figure displays the average absolute concentrations of VOCs in the five sampling points, with dashed lines representing the average values.

As the flowers bloomed, the ***OFP*** of benzyl alcohol and phenol increased while that of benzaldehyde decreased. Other volatiles exhibited fluctuating trends (Table 2). Overall, the ***OFP*** of *M. azedarach* exhibited distinct phases: total VOC emission values were 4.881 μg/m^3, 13.464 μg/m^3, and 17.683 μg/m^3 and peaked during SH. This trend correlated with heightened plant physiological and metabolic activity. The contribution of dominant compounds also varied significantly across stages: ethanol dominated DL (94.63%) and remained predominant during CH (81.28%). During SH, phenol became the largest contributor (54.04%) and the contribution of ethanol decreased to 40.23%. Notably, benzaldehyde exhibited a negative ***OFP*** value, which indicates an ozone-suppressing effect that was pronounced during SH.

Table 2. ***OFP*** of VOCs from *M. azedarach* road at different flowering stages.

VOCs	MIR	*OFP* (μg/m^3)			Contribution Ratio to Ozone Generation (%)		
		DL	CH	SH	DL	CH	SH
1-Hexanol	2.69	-	1.272	0.527	-	9.447	2.980
1-Octanol	1.43	-	0.183	-	-	1.359	-
Ethanol	1.53	4.619	10.944	0.771	94.632	81.283	40.225
Benzyl alcohol	5.11	-	1.686	9.556	-	12.522	1.374
Benzaldehyde	−0.67	−0.132	−0.666	−7.113	−2.704	−4.947	−4.360
Phenol	2.76	0.130	0.168	0.243	2.663	1.248	54.041
Total	-	4.881	13.464	17.683	100	100	100

3.3. BVOCs from M. grandiflora Flowers and Their Release into Roadside Air

3.3.1. Analysis of Volatile Types and Absolute Concentrations

A total of 64 volatiles from *M. grandiflora* flowers were identified and categorized into nine groups, including esters, olefins, and alkanes. As shown in Figure 2, the absolute concentration of terpenoids accounted for the highest proportion among all components, respectively accounting for 22.22%, 45.45%, and 47.37% during the DL, CH and SH phases. The absolute concentration proportion of aldehydes, alkanes, aromatic hydrocarbons, and ketones gradually decreased. According to Appendix A Table A3, nerolidol was the volatile with the highest concentration during CH, while that of phenethyl alcohol was the highest during SH. The absolute concentration of aldehydes such as phenylacetaldehyde and alcohols like leaf alcohol gradually increased. Other volatiles exhibited pronounced fluctuation.

Ten volatiles were common across flowering stages in *M. grandiflora*. Fifteen unique compounds appeared during DL, ten unique compounds appeared during CH, and fifteen unique compounds appeared during SH (Figure 7). Among the ten common compounds, the absolute concentration of phenylacetaldehyde gradually increased, while that of n-pentadecane gradually decreased. The absolute concentrations of the remaining eight volatiles fluctuated. Among the unique volatiles, twelve volatiles were identified during CH and SH. The absolute concentrations of benzyl alcohol, a mixture of isomers, (-)-alpha-phellandrene, trans-caryophyllene, and methyl hexanoate increased as the flowers bloomed, while the other seven volatiles decreased.

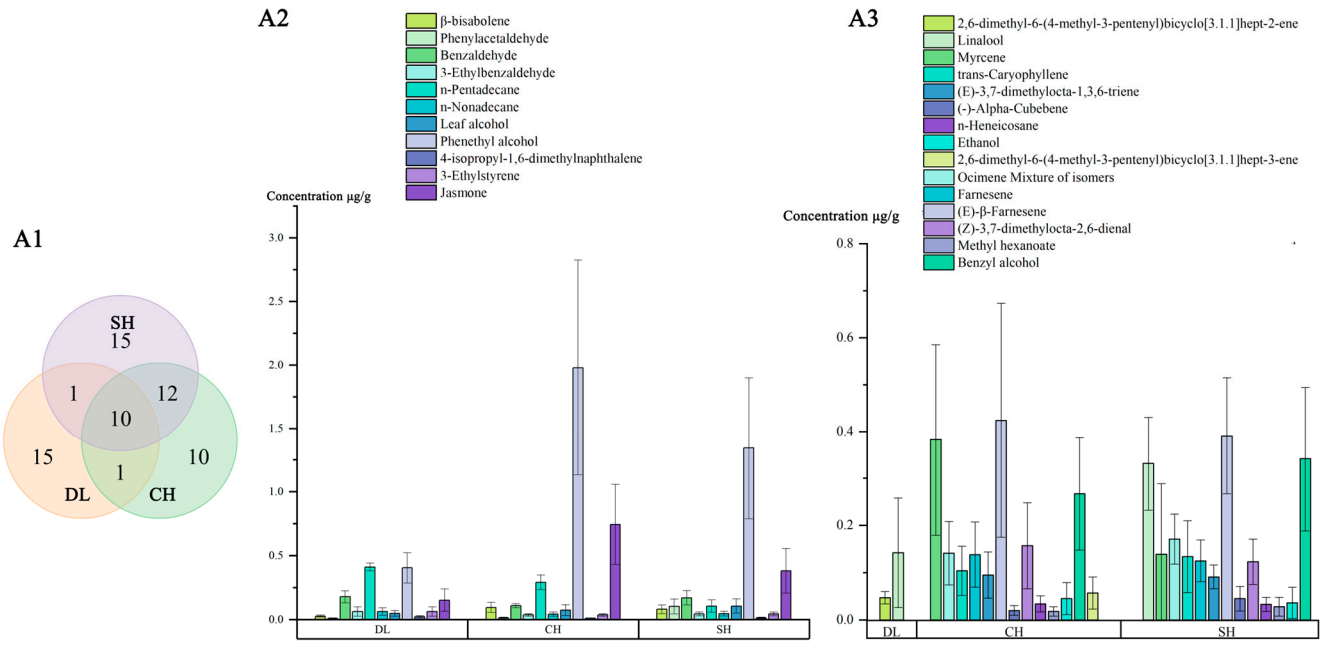


Figure 7. Types and absolute concentration of BVOCs at different flowering stages of *M. grandiflora*. The numbers in the (**A1**) overlapping sections represent the types of components common to different periods, while the non-overlapping sections indicate the types of components unique to that period. In (**A2**) we see the absolute concentration of common volatiles and (**A3**) shows the absolute concentration of unique volatiles at different flowering stages.

3.3.2. Release of VOCs into Roadside Air

Fifteen target volatiles were detected at sampling points along the roadside. Average concentrations ranged from 3.722–54.972 μg/m^3. Overall, terpenes constituted the highest proportion of volatiles in the roadside air and accounted for 33.25% of all target volatiles. Among terpenes, linalool exhibited the highest concentration (Figure 8).

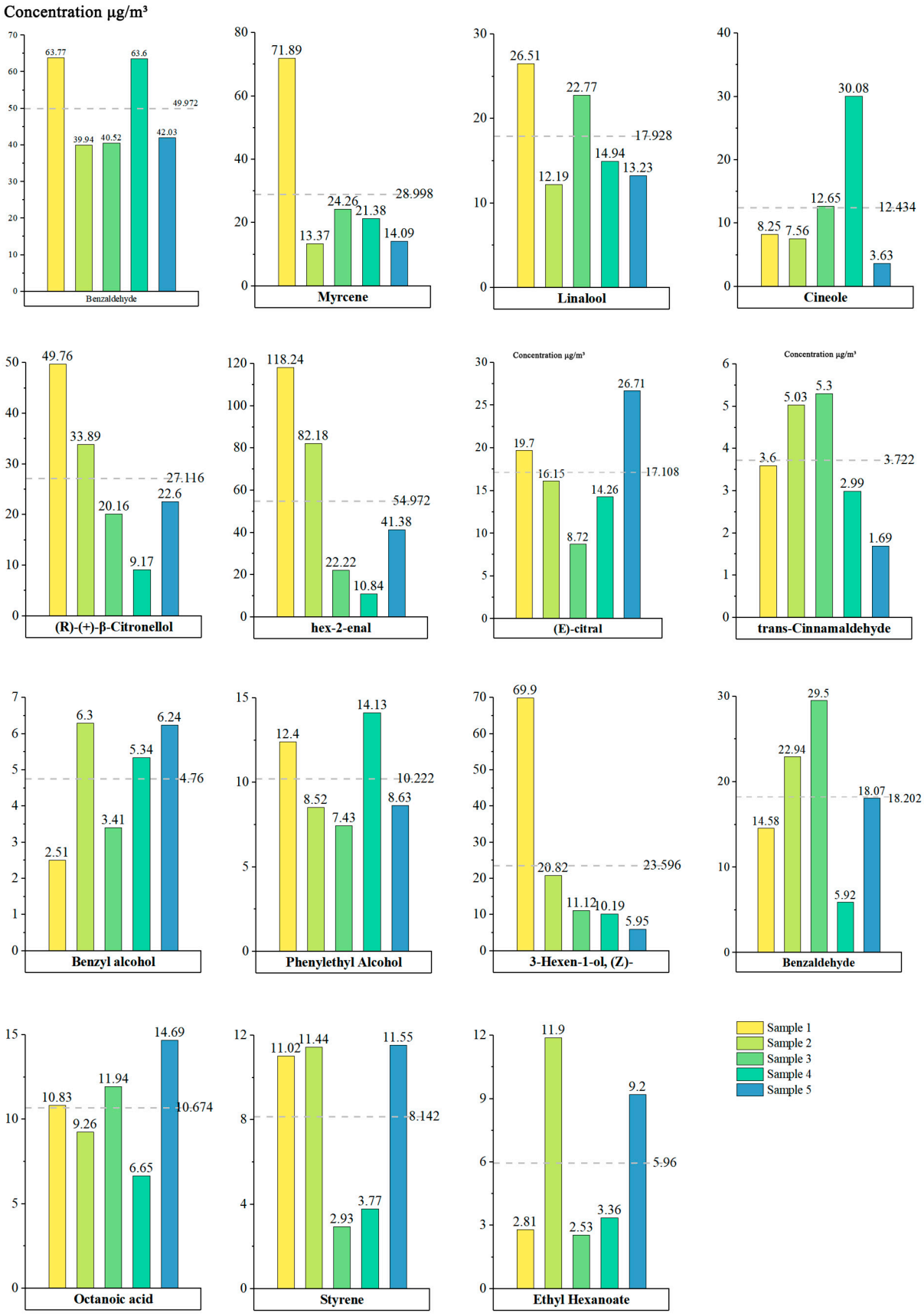


Figure 8. Fifteen target VOCs in roadside air with *M. grandiflora*. The figure displays the average absolute concentrations of VOCs in the five sampling points, with dashed lines representing the average values.

During different stages, the total values for VOC emission were −0.120 μg/m^3, 1.505 μg/m^3, and 1.912 μg/m^3 (Table 3). This trend indicates that, as the flowers bloomed, emissions shifted from inhibiting to promoting ozone formation, and a particularly significant increase in the ***OFP*** occurred from the CH to SH. Benzaldehyde—the sole compound with a negative MIR value—emerged as the only active compound during DL and exhibited a pronounced ozone-suppressing effect. Upon reaching CH and SH, the ozone-suppressing effect of benzaldehyde was surpassed by the ozone-promoting effects of ethanol and benzyl alcohol. Notably, benzyl alcohol dominated DL and SH, in which it contributed 91.161% and 90.631%, respectively, to the ***OFP***, while the contribution of ethanol was relatively minor.

Table 3. ***OFP*** of VOCs from roadside *M. grandiflora* at different flowering stages.

VOCs	MIR	*OFP* (μg/m^3)			Contribution Ratio to Ozone Generation (%)		
		DL	CH	SH	DL	CH	SH
Benzaldehyde	−0.67	−0.120	−0.072	−0.114	−100.000	−5.962	−4.784
Ethanol	1.53	-	0.069	0.055	-	2.877	4.585
Benzyl alcohol	5.11	-	1.364	1.743	-	91.161	90.631
Total	-	−0.120	1.505	1.912	100	100	100

4. Discussion

4.1. Detection and Analysis of BVOCs from Fragrant Flowering Trees

HS–SPME and GC–MS were employed to identify BVOCs from *P. tomentosa*, *M. azedarach*, and *M. grandiflora* flowers at three flowering stages. These species are commonly planted as street trees in Shanghai. Previously, 45 floral volatiles were identified from *P. tomentosa* [34], and alcohols (primarily 1-octen-3-ol and 3-octanol) were the most abundant group of volatiles, which is consistent with the present results. Different methods have been employed to analyze the volatiles of floral essential oils from these three species [31–33], and the compounds identified previously are similar to those identified in the present study, though they varied in content. Differences between previous studies and the present research may be due to variation in plant varieties, origins, extraction methods, or analytical instrument parameters. In our study, the types and concentrations of volatiles at different flowering stages were screened comprehensively, and the number of volatiles in the floral parts of the three species gradually increased as the flowers bloomed. In *P. tomentosa*, 35 volatiles were identified during SH compared with 22 during DL and 29 during CH, but alcohols dominated in all stages. In *M. azedarach*, 29 volatiles were identified during SH compared with 21 during CH and only 13 during DL, and the absolute concentration of alcohols accounted for the highest proportion among all components during the DL and CH, while that of terpenes became predominant during the SH. In *M. grandiflora*, 38 volatiles were identified during SH compared with 33 during CH and 27 during DL. Volatiles in DL, CH and SH were dominated by terpenes. Differences in the number and concentration of volatiles at different flowering stages may be related to physiological metabolic changes during floral development.

4.2. Health Benefits and Applications of BVOCs from Fragrant Flowering Trees

Researchers have identified certain BVOCs in plant essential oils and extracts that exhibit antibacterial, antioxidant, and anti-inflammatory properties, indicating that these three fragrant street trees possess resource potential as health-promoting plants. Floral volatiles offer certain health benefits to humans. Previously, linalool from *P. tomentosa* was shown to have multiple physiological effects including antioxidant, anti-inflammatory, analgesic, neuroprotective, and antibacterial effects [35]. Citral has been shown to possess antibacterial and anti-inflammatory properties [36]. β-bisabolene demonstrates sooth-

ing, sedative, anti-inflammatory, anti-itch, anti-allergic, and nerve-nourishing effects [37]. (E)-β-Acaciaene has anticancer, neuroprotective, and antioxidant properties. Geranylacetone demonstrates antioxidant, anti-inflammatory, and antibacterial effects [38]. Acaciaenol possesses antibacterial activity [39]. Among the main volatiles from *P. tomentosa*, 1-octen-3-ol has potential applications for pathogen control [40], methyl salicylate exhibits antibacterial activity [41], and methyl eugenol exhibits analgesic, anesthetic, anti-allergic, anti-inflammatory, antioxidant, and antitumor effects.

Among the floral volatiles of *M. azedarach* at different flowering stages, ziziphenone has antibacterial, analgesic, and anti-inflammatory activities [42]. Ethanol and jasmone exhibit antibacterial effects [42]. β-caryophyllene has diverse pharmacological activities, including antioxidant, anti-inflammatory, and anti-apoptotic properties. Nerolidol demonstrates pharmacological and biological activities, such as antioxidant and anti-inflammatory effects, and it is commonly used as an antimicrobial agent.

For the floral volatiles of *M. grandiflora*, numerous compounds exhibit bactericidal and antimicrobial effects, such as trans-cinnamaldehyde, which also possesses disinfectant and antiviral properties [43]. Geraniol and α-santalene demonstrate antioxidant, antibacterial, and anti-inflammatory effects [44]. Perillic acid exhibits antibacterial and antitumor effects [44]. (-)-alpha-guaiene and Δ-juniperene possess antibacterial and antioxidant activity [45]. β-cercarene demonstrates antibacterial, antioxidant, and anti-inflammatory properties [46]. Eucalyptol exhibits anti-inflammatory and antioxidant effects [47]. Farnesol modulates intercellular communication, effectively treats metabolic disorders, and exhibits anti-inflammatory, antioxidant, antitumor, and antibacterial activities [39]. Among the major volatiles of *M. grandiflora*, linalool [48] and phenethyl alcohol have demonstrated notable antibacterial effects against multiple bacterial strains. However, there may be differences in whether the same compounds found in essential oils and other extracts and those present as VOCs in roadside air produce equivalent physiological effects. Therefore, their actual health benefits (such as antibacterial and anti-inflammatory effects) in urban road environments still require confirmation through subsequent cell experiments, animal models, or population epidemiological studies.

4.3. Ecological and Therapeutic Value of BVOCs Emitted from Fragrant Flowering Trees to the Roadside Air

BVOCs emitted by flowering trees along roadsides may affect air quality and human emotions. Volatile compounds such as benzaldehyde, eugenol, and methyl salicylate contribute to air purification [49,50]. Numerous studies have demonstrated that plant volatiles such as isoprene and monoterpenes play a key role in promoting ozone formation [51,52]. In this study, we calculated the ***OFP*** of target volatiles emitted into the air by flowering street trees with the goal of quantifying their effect on air quality and providing a scientific basis for the selection of urban flowering street trees. We found that the ***OFP*** of *P. tomentosa*, *M. azedarach*, and *M. grandiflora* exhibited distinct temporal patterns across different flowering stages. Overall, from DL to SH, enhanced plant metabolic activity increased the emission of most BVOCs and increased the ***OFP***. However, the ***OFP*** for a small number of volatiles fluctuated and was correlated with environmental factors such as temperature, solar radiation, and light exposure [53].

BVOCs along roadsides may also influence the physiological and psychological states of humans. For example, 1-octen-3-ol possesses a mushroom-like aroma, (R)-citronellol promotes digestion and soothes muscles and the nervous system [54], and cis-3-hexen-1-ol (geraniol) carries a strong grassy scent [55] and exerts a positive mood-regulating effect on humans. Artemisinone is a bioactive compound or active intermediate with antidepressant, stress-relieving, stomach-strengthening, and mind-awakening functions [56]. cis-α-Bisabolene and β-Bisabolene benefit the nervous system by improving mood and

cognitive function, and these compounds assist in alleviating psychological issues such as anxiety and depression [57]. Linalool stimulates the central nervous system to relieve mental fatigue and refresh the mind, while its naturally fresh scent helps relax tense nerves. In contrast, certain compounds exert negative effects on human mood and physiology. For instance, benzene compounds exhibit strong toxicity and carcinogenicity, irritate the skin and mucous membranes, and damage the respiratory, hematopoietic, and nervous systems [58]. The pungent odor of benzaldehyde may induce irritability and tension [59]. Prolonged exposure to high benzaldehyde concentrations may cause skin allergies or affect the central nervous system, necessitating the avoidance of areas with a high concentration of this compound [60].

4.4. Limitations and Future Research Directions

The target volatiles were selected based on the SIFT–MS built-in database, and only 12 volatiles from *P. tomentosa*, 7 from *M. azedarach*, and 14 from *M. grandiflora* were selected for evaluation of emission to the environment. The release of other identified floral volatiles into the air could not be analyzed, which prevented a comprehensive assessment of floral volatile compound emissions. When sampling air along roads lined with flowering trees, the roads where *P. tomentosa* grow also feature *Ophiopogon japonicus* (L. f.) Ker Gawl., *Photinia* × *fraseri* Dress, and *Ligustrum lucidum* W. T. Aiton. Although sampling was conducted within a 1 m radius beneath the flowering trees, it is impossible to completely rule out the influence of BVOC emissions from these nearby trees on the collected air samples. Furthermore, this study calculated the ***OFP*** of BVOCs released during the flowering period of trees based on BVOC concentrations and MIR. This approach simplifies complex atmospheric chemistry into an idealized linear contribution model. The results primarily reflect the theoretical maximum reactivity of specific BVOCs under controlled laboratory conditions, failing to capture the impact of dynamic, nonlinear synergistic reactions between NO_x produced mainly by vehicles on the road and BVOCs in actual road environments on ***OFP***. Therefore, this constitutes a static assessment. Future research should focus on dynamic assessments that incorporate real-time environmental parameters such as NO_x, VOCs, temperature, wind speed, etc., to more accurately quantify the contribution of VOCs to ozone formation in real-world environments.

5. Conclusions

We investigated the composition and characteristics of volatiles from three commonly used species of fragrant flowering street trees in Shanghai and evaluated emission patterns in roadside air and the potential health benefits of BVOCs. This study systematically integrated the assessment of floral volatiles, BVOC emissions into roadside air, and ***OFP*** at different flowering stages of flowering street trees. It established a comprehensive analytical chain that spans from flowers to roadside air to environmental impacts and health effects, offering a novel integrated research paradigm for understanding the dynamics of BVOCs emitted by urban street trees. The results demonstrate the following: (1) The main volatiles from *P. tomentosa* flowers were alcohols (e.g., 1-octen-3-ol) and phenolic ethers (e.g., eugenol and methyl eugenol), the main volatiles from *azedarach* were alcohols (e.g., ethanol) and aldehydes (e.g., benzaldehyde), and the main volatiles from *M. grandiflora* were terpenes (e.g., (E)-β-aacacene). (2) As flowers bloomed, the diversity and concentration of volatiles significantly increased in all three species, thus reflecting heightened metabolic activity during floral development. (3) The characteristics of volatiles emitted to roadside air were consistent with those of the flowers: alcohols dominated in the air near *P. tomentosa* and *M. azedarach*, with 1-octen-3-ol reaching the highest concentration at the *P. tomentosa* site and phenethyl alcohol dominating at the *M. azedarach* site. Terpenes and aldehydes dominated

at the *M. grandiflora* site. Emissions of most BVOCs gradually increased throughout the flowering period and contributed directly to an elevated ***OFP***. (4) BVOCs identified in flowers and roadside air contain bioactive compounds with antibacterial, antioxidant, and anti-inflammatory properties (such as eugenol, trans-cinnamaldehyde, and (E)-β-farnesene) in related studies of plant essential oils, thus demonstrating the potential value of street trees in public health. By combining HS–SPME, GC–MS, and SIFT–MS techniques, we systematically analyzed volatiles emitted from floral parts to the ambient air, which is an effective pathway for studying plant volatiles in the environment. These findings provide a scientific basis for refining urban roadside green spaces to balance ecological services and health benefits. A better understanding of BVOCs will enable urban managers to prioritize healthier and more sustainable development of urban roadsides.

Author Contributions: X.W.: Conceptualization, methodology, formal analysis, investigation, writing—original draft preparation, visualization. Y.W.: Conceptualization, methodology, validation, investigation. Y.Z. (Yanting Zhang): Supervision, resources. R.Y.: Project administration, funding acquisition. M.F.: Data curation, visualization, investigation. B.W.: Resources, editing. Y.Z. (Yali Zhang): Resources, writing—review and editing, supervision, funding acquisition. M.W.: Resources, writing—review and editing, supervision. All authors have read and agreed to the published version of the manuscript.

Funding: This research was funded by the Agriculture Research System of Shanghai, China, grant number 2025-8-03, 2023 Shanghai Oriental Talents Program—Youth Project, grant number Shanghai Talent [2024] No. 4, the Shanghai Academy of Agricultural Sciences Program for Excellent Research Team (2025-030) and the Special Fund Project for Construction of Engineering Technology Research Center of Shanghai Municipal Science and Technology Commission (No. 17DZ2252000).

Institutional Review Board Statement: Not applicable.

Informed Consent Statement: Not applicable.

Data Availability Statement: The datasets supporting the results presented in this manuscript are included within the article.

Acknowledgments: The authors acknowledge the support of all the interview participants.

Conflicts of Interest: The authors declare no conflicts of interest.

Abbreviations

The following abbreviations are used in this manuscript:

HS–SPME	Headspace-sampling solid-phase microextraction
GC–MS	Gas chromatography–mass spectrometry
SIFT–MS	Selected-ion flow-tube mass spectrometry
BVOCs	Biogenic volatile organic compounds
OFP	Ozone formation potential
DL	Bud stage
CH	Initial bloom stage
SH	Bloom stage

Appendix A

Table A1. The table shows BVOCs in the floral parts of *P. tomentosa* throughout the flowering period: DL: Bud stage, CH: Initial bloom stage, SH: Bloom stage.

	BVOC	Molecular Formula	Concentration µg/g		
			DL	CH	SH
Alcohols (7)					
1	1-octen-3-ol *	$C_8H_{18}O$	2.403 ± 1.007	4.04 ± 0.606	1.083 ± 0.133
2	(±)-octan-3-ol #	$C_{13}H_{24}O$	-	0.274 ± 0.068	-
3	6,10-dimethylundeca-5,9-dien-2-ol	C_7H_8O	-	0.016 ± 0.006	0.05 ± 0.013
4	Benzyl alcohol *	$C_8H_{10}O$	0.017 ± 0.01	0.075 ± 0.052	0.092 ± 0.01
5	Phenylethyl Alcohol	$C_6H_{12}O$	0.008 ± 0.002	0.013 ± 0.007	-
6	3-Hexen-1-ol, (Z)- *	$C_6H_{14}O$	0.058 ± 0.028	0.066 ± 0.019	0.046 ± 0.006
7	1-Hexanol	$C_{14}H_{22}O$	-	0.069 ± 0.02	0.03 ± 0
Phenols (7)					
8	Phenol, 2,5-bis(1,1-dimethylethyl)- #	$C_8H_{10}O_2$	0.02 ± 0.003	-	-
9	Creosol	$C_9H_{10}O$	-	0.029 ± 0.011	0.021 ± 0.004
10	p-Allylphenol #	C_6H_6O	-	-	0.047 ± 0.031
11	Phenol	$C_{10}H_{12}O_2$	0.005 ± 0.002	0.015 ± 0.005	-
12	Eugenol *	$C_{10}H_{12}O_2$	0.023 ± 0.015	0.095 ± 0.037	0.334 ± 0.074
13	trans-Isoeugenol	$C_{11}H_{14}O_2$	-	-	0.062 ± 0.017
14	Methyleugenol *	$C_9H_{12}O_3$	0.021 ± 0.01	0.122 ± 0.056	0.395 ± 0.048
Ethers (5)					
15	1,2,4-Trimethoxybenzene *	$C_8H_{10}O_2$	0.007 ± 0.004	0.041 ± 0.025	0.222 ± 0.053
16	Benzene, 1,4-dimethoxy- #	$C_8H_{10}O$	-	-	0.107 ± 0.033
17	4-Methylanisole #	$C_{10}H_{12}O$	-	-	0.01 ± 0.003
18	Anethole *	$C_{11}H_{14}O_2$	0.011 ± 0.006	0.097 ± 0.036	0.128 ± 0.042
19	Benzene,1,2-dimethoxy-4-(1-propenyl)- *	$C_8H_{10}O_2$	0.025 ± 0.012	0.159 ± 0.087	0.736 ± 0.153
Aldehydes (6)					
20	2,4-Hexadienal #	$C_6H_{10}O$	-	-	0.011 ± 0.001
21	2-Hexenal *	C_7H_6O	0.064 ± 0.03	0.099 ± 0.053	0.066 ± 0.006
22	Benzaldehyde *	$C_{10}H_{16}O$	0.016 ± 0.005	0.048 ± 0.018	0.042 ± 0.004
23	Citral #	$C_7H_6O_2$	-	-	0.006 ± 0
24	Salicylaldehyde	$C_6H_{12}O$	-	0.011 ± 0.008	0.037 ± 0.016
25	Hexanal	$C_{10}H_{16}$	0.04 ± 0.027	-	0.027 ± 0.002
Terpenes (6)					
26	1,3,6-Octatriene, 3,7-dimethyl-, (Z)-	$C_{15}H_{24}$	-	0.014 ± 0.005	0.043 ± 0.007
27	(E)-β-Farnesene	$C_{15}H_{24}$	-	0.101 ± 0.037	0.107 ± 0.023
28	β-Bisabolene	$C_{15}H_{26}O$	-	0.008 ± 0.002	0.011 ± 0.002
29	Nerolidol	$C_{15}H_{26}O$	0.047 ± 0.037	-	0.187 ± 0.052
30	trans-Farnesol	$C_{13}H_{22}O$	-	0.164 ± 0.013	-
31	5,9-Undecadien-2-one,6,10-dimethyl-, (E)-	$C_8H_{16}O$	0.047 ± 0.038	0.197 ± 0.07	-

Table A1. *Cont.*

	BVOC	Molecular Formula	Concentration μg/g		
			DL	CH	SH
Ketones (3)					
32	3-Octanone *	$C_8H_{12}O$	0.067 ± 0.037	0.101 ± 0.015	0.071 ± 0.005
33	6-Methyl-3,5-heptadiene-2-one #	$C_{18}H_{36}O$	-	-	0.007 ± 0.002
34	2-Pentadecanone, 6,10,14-trimethyl-	$C_{27}H_{56}$	0.018 ± 0.007	-	0.042 ± 0.028
Alkanes (7)					
35	Heptacosane #	$C_{20}H_{42}$	-	-	0.016 ± 0.015
36	Icosane #	$C_{21}H_{44}$	-	-	0.009 ± 0.004
37	Heneicosane #	$C_{12}H_{26}$	-	-	0.004 ± 0.002
38	Dodecane	$C_{16}H_{34}$	-	0.013 ± 0.003	0.005 ± 0.001
39	Hexadecane *	$C_{13}H_{28}$	0.005 ± 0.001	0.012 ± 0.004	0.01 ± 0.007
40	Tridecane #	$C_{11}H_{24}$	-	0.022 ± 0.005	-
41	Undecane #	$C_{14}H_{12}O_2$	0.005 ± 0.003	-	-
Esters (2)					
42	Benzyl Benzoate	$C_8H_8O_3$	0.031 ± 0.018	0.29 ± 0.15	-
43	Methyl salicylate *	C_8H_{12}	0.104 ± 0.022	0.512 ± 0.316	0.114 ± 0.044
Others (2)					
44	1,2-Dimethyl-Δ3,5-cyclohexadien #	$C_{12}H_{16}O_3$	-	0.044 ± 0.021	-
45	Elemicin #	$C_8H_{16}O$	-	-	0.011 ± 0.002

Note: * indicates compounds appear in 3 flowering periods of *P. tomentosa*. # indicates compounds appear in the specific flowering period; - indicates the compound was not detected in that flowering period.

Table A2. The table shows BVOCs in the floral parts of *M. azedarach* throughout the flowering period: DL: Bud stage, CH: Initial bloom stage, SH: Bloom stage.

	BVOC	Molecular Formula	Concentration μg/g		
			DL	CH	SH
	Alcohols (7)				
1	1-Hexanol	$C_6H_{14}O$	-	0.473 ± 0.308	0.196 ± 0.121
2	1-Octanol #	$C_8H_{18}O$	-	0.128 ± 0.093	-
3	3-Hexanol	$C_6H_{14}O$	-	1.622 ± 1.433	0.101 ± 0.03
4	Ethyl alcohol *	C_2H_6O	3.019 ± 2.269	7.153 ± 5.079	0.504 ± 0.245
5	1-Nonanol #	$C_9H_{20}O$	0.085 ± 0.053	-	-
6	Phenylethyl Alcohol *	$C_8H_{10}O$	0.107 ± 0.077	1.835 ± 1.341	7.938 ± 6.056
7	1-Butanol, 3-methyl- #	$C_5H_{12}O$	0.247 ± 0.196	-	-
8	3-Hexen-1-ol, (Z)- *	$C_6H_{12}O$	0.754 ± 0.554	0.429 ± 0.214	0.122 ± 0.081
9	Benzyl Alcohol	C_7H_8O	-	0.33 ± 0.155	1.87 ± 0.881
10	3-Phenyl-1-propanol #	$C_9H_{12}O$	-	-	0.07 ± 0.021
11	2-Methoxybenzyl alcohol #	$C_8H_{10}O_2$	-	-	0.409 ± 0.103

Table A2. *Cont.*

	BVOC	Molecular Formula	Concentration μg/g		
			DL	CH	SH
	Aldehydes (8)				
12	trans-2-Nonenal #	$C_9H_{16}O$	-	-	0.13 ± 0.093
13	Benzaldehyde *	C_7H_6O	0.197 ± 0.097	0.994 ± 0.354	10.616 ± 11.189
14	Nonanal *	$C_9H_{18}O$	0.624 ± 0.433	0.544 ± 0.348	0.317 ± 0.151
15	2-Hexenal *	$C_6H_{10}O$	0.569 ± 0.264	0.406 ± 0.197	0.444 ± 0.51
16	Phenylacetaldehyde	C_8H_8O	-	1.162 ± 0.933	2.678 ± 2.62
17	o-Anisaldehyde	$C_8H_8O_2$	-	0.049 ± 0.014	0.748 ± 0.566
18	4-methoxy-Benzaldehyde #	$C_8H_8O_2$	-	-	0.23 ± 0.1
19	trans,trans-2,4-Heptadienal #	$C_7H_{10}O$	-	-	0.037 ± 0.031
	Terpenes (6)				
20	(E)-β-Farnesene	$C_{15}H_{24}$	-	0.32 ± 0.161	1.809 ± 0.72
21	β-Elemene #	$C_{15}H_{24}$	-	0.08 ± 0.034	-
22	β-Caryophyllene *	$C_{15}H_{24}$	1.346 ± 0.629	2.17 ± 1.101	0.328 ± 0.108
23	β-bisabolene	$C_{15}H_{24}$	-	0.067 ± 0.034	0.296 ± 0.108
24	5,9-Undecadien-2-one, 6,10-dimethyl-, (E)-	$C_{13}H_{22}O$	-	0.027 ± 0.036	0.212 ± 0.092
25	Nerolidol #	$C_{15}H_{26}O$	-	-	10.412 ± 3.042
	Ethers (3)				
26	Benzene, 1,4-dimethoxy- *	$C_8H_{10}O_2$	0.368 ± 0.325	3.982 ± 3.401	5.671 ± 0.47
27	1,2,4-Trimethoxybenzene #	$C_9H_{12}O_3$	-	-	0.143 ± 0.022
28	Estragole #	$C_{10}H_{12}O$	-	-	0.067 ± 0.014
	Ketones (2)				
29	2-Pentadecanone, 6,10,14-trimethyl-	$C_{18}H_{36}O$	-	0.103 ± 0.059	0.073 ± 0.038
30	1,2-Propanedione, 1-phenyl- #	$C_9H_8O_2$	-	-	0.562 ± 0.122
	Esters (2)				
31	Methyl salicylate #	$C_8H_8O_3$	0.037 ± 0.018	-	-
32	Methyl cinnamate #	$C_{10}H_{10}O_2$	-	-	0.063 ± 0.038
	Phenols (1)				
33	Phenol *	C_6H_6O	0.047 ± 0.025	0.061 ± 0.035	0.088 ± 0.084
	Alkanes (1)				
34	Undecane *	$C_{11}H_{24}$	0.09 ± 0.058	0.116 ± 0.085	0.05 ± 0.035

Note: * indicates compounds appear in 3 flowering periods of *M. azedarach*. # indicates compounds appear in the specific flowering period; - indicates the compound was not detected in that flowering period.

Table A3. The table shows BVOCs in the floral parts of *M. grandiflora* throughout the flowering period: DL: Bud stage, CH: Initial bloom stage, SH: Bloom stage.

	BVOC	Molecular Formula	Concentration μg/g		
			DL	CH	SH
	Terpenes (28)				
1	Perillen #	$C_{10}H_{14}O$	-	0.036 ± 0.025	-
2	Myrcene	$C_{10}H_{16}$	-	0.382 ± 0.203	0.139 ± 0.149

Table A3. *Cont.*

	BVOC	Molecular Formula	Concentration µg/g		
			DL	CH	SH
3	Geranylacetone #	$C_{13}H_{22}O$	-	-	0.113 ± 0.045
4	(Z)-α-bisabolene #	$C_{15}H_{24}$	-	-	0.206 ± 0.119
5	Ocimene Mixture of isomers	$C_{10}H_{16}$	-	0.141 ± 0.067	0.171 ± 0.053
6	Linalool	$C_{10}H_{18}O$	0.142 ± 0.116	-	0.331 ± 0.099
7	trans-Caryophyllene	$C_{15}H_{24}$	-	0.104 ± 0.052	0.134 ± 0.076
8	trans-nerolidol #	$C_{15}H_{26}O$	-	-	0.377 ± 0.612
9	Farnesol #	$C_{15}H_{26}O$	-	-	0.377 ± 0.548
10	Nerolidol #	$C_{15}H_{26}O$	-	2.527 ± 1.355	-
11	1,6,10-Dodecatrien-3-ol, 3,7,11-trimethyl- #	$C_{15}H_{26}O$	0.078 ± 0.078	-	-
12	Neo-Alloocimene,stab #	$C_{10}H_{16}$	-	-	0.02 ± 0.007
13	Cineole #	$C_{10}H_{18}O$	-	-	0.017 ± 0.011
14	Delta-Cadinene #	$C_{15}H_{24}$	-	-	0.057 ± 0.029
15	γ-Muurolene #	$C_{15}H_{24}$	0.005 ± 0.003	-	-
16	p-mentha-1(7),2-diene #	$C_{10}H_{16}$	-	-	0.034 ± 0.01
17	β-bisabolene *	$C_{15}H_{24}$	0.027 ± 0.008	0.095 ± 0.039	0.081 ± 0.034
18	α-ylangene #	$C_{15}H_{24}$	0.025 ± 0.009	-	-
19	2,6-dimethyl-6-(4-methyl-3-pentenyl)bicyclo[3.1.1]hept-2-ene	$C_{15}H_{24}$	0.047 ± 0.013	0.057 ± 0.034	-
20	Santalene #	$C_{15}H_{24}$	-	0.01 ± 0.003	-
21	Farnesene	$C_{15}H_{24}$	-	0.138 ± 0.069	0.125 ± 0.044
22	(Z,E)-α-Farnesene #	$C_{15}H_{24}$	-	0.076 ± 0.046	-
23	(R)-(+)-β-Citronellol #	$C_{10}H_{20}O$	-	-	0.071 ± 0.033
24	(E)-3,7-dimethylocta-1,3,6-triene	$C_{10}H_{16}$	-	0.095 ± 0.049	0.091 ± 0.025
25	(E)-β-Farnesene	$C_{15}H_{24}$	-	0.424 ± 0.249	0.391 ± 0.124
26	(2E,4E,6E)-3,4-Dimethyl-2,4,6-Octatriene #	$C_{10}H_{16}$	-	0.016 ± 0.011	-
27	(-)-alpha-Gurjunene #	$C_{15}H_{24}$	-	0.079 ± 0.036	-
28	(-)-Alpha-Cubebene	$C_{15}H_{24}$	-	0.02 ± 0.01	0.045 ± 0.026
	Aldehydes (11)				
29	(2E,6E)-3,7,11-trimethyldodeca-2,6,10-trienal #	$C_{15}H_{24}O$	-	-	0.109 ± 0.037
30	trans-Cinnamaldehyde #	C_9H_8O	-	0.01 ± 0.002	-
31	Trans-2-Hexenal #	$C_6H_{10}O$	0.026 ± 0.006	-	-
32	p-Tolualdehyde #	C_8H_8O	0.073 ± 0.033	-	-
33	Phenylacetaldehyde *	C_8H_8O	0.009 ± 0.005	0.014 ± 0.004	0.103 ± 0.058
34	Benzaldehyde *	C_7H_6O	0.178 ± 0.047	0.108 ± 0.016	0.17 ± 0.056
35	4-Ethylbenzaldehyde #	$C_9H_{10}O$	0.068 ± 0.025	-	-

Table A3. *Cont.*

	BVOC	Molecular Formula	Concentration μg/g		
			DL	CH	SH
36	3-Ethylbenzaldehyde *	$C_9H_{10}O$	0.063 ± 0.037	0.037 ± 0.01	0.045 ± 0.015
37	hex-2-enal #	$C_6H_{10}O$	-	0.031 ± 0.02	-
38	(Z)-3,7-dimethylocta-2,6-dienal	$C_{10}H_{16}O$	-	0.157 ± 0.091	0.123 ± 0.048
39	(E)-citral #	$C_{10}H_{16}O$	-	-	0.61 ± 0.192
	Alkanes (6)				
40	n-Pentadecane *	$C_{15}H_{32}$	0.411 ± 0.03	0.29 ± 0.057	0.106 ± 0.048
41	n-Heptadecane #	$C_{17}H_{36}$	0.039 ± 0.009	-	-
42	n-Nonadecane *	$C_{19}H_{40}$	0.063 ± 0.029	0.043 ± 0.017	0.046 ± 0.018
43	n-Heneicosane	$C_{21}H_{44}$	-	0.034 ± 0.017	0.033 ± 0.015
44	n-Hendecane #	$C_{11}H_{24}$	0.004 ± 0.001	-	-
45	Tetradecane #	$C_{14}H_{30}$	0.015 ± 0.004	-	-
	Esters (6)				
46	Ethyl Hexanoate #	$C_8H_{16}O_2$	-	-	0.1 ± 0.071
47	Methyl Laurate #	$C_{13}H_{26}O_2$	0.027 ± 0.007	-	-
48	Benzyl Caprylate #	$C_{15}H_{22}O_2$	-	-	0.037 ± 0.02
49	Octanoic acid, 2-phenylethyl ester #	$C_{16}H_{24}O_2$	-	-	0.138 ± 0.108
50	Methyl hexanoate	$C_7H_{14}O_2$	-	0.018 ± 0.01	0.028 ± 0.02
51	Benzylcarbinyl caproate #	$C_{14}H_{20}O_2$	-	-	0.097 ± 0.066
	Alcohols (4)				
52	Ethanol	C_2H_6O	-	0.045 ± 0.034	0.036 ± 0.033
53	Leaf alcohol *	$C_6H_{12}O$	0.049 ± 0.022	0.074 ± 0.042	0.106 ± 0.056
54	Phenethyl alcohol *	$C_8H_{10}O$	0.404 ± 0.119	1.978 ± 0.847	1.343 ± 0.556
55	Benzyl alcohol	C_7H_8O	-	0.267 ± 0.119	0.341 ± 0.153
	Aromatic hydrocarbons (4)				
56	4-isopropyl-1,6-dimethylnaphthalene *	$C_{15}H_{18}$	0.022 ± 0.009	0.011 ± 0.001	0.014 ± 0.005
57	Styrene #	C_8H_8	0.027 ± 0.007	-	-
58	4-Ethylstyrene #	$C_{10}H_{12}$	0.054 ± 0.038	-	-
59	3-Ethylstyrene *	$C_{10}H_{12}$	0.063 ± 0.037	0.037 ± 0.01	0.045 ± 0.015
	Acids (2)				
60	Octanoic acid #	$C_8H_{16}O_2$	-	0.101 ± 0.06	-
61	Geranic acid #	$C_{10}H_{16}O_2$	-	0.115 ± 0.097	-
	Olefins (2)				
62	Cyclopentadecane #	$C_{15}H_{30}$	0.017 ± 0.005	-	-
63	8-Heptadecene #	$C_{17}H_{34}$	0.012 ± 0.003	-	-
	Ketones (1)				
64	Jasmone *	$C_{11}H_{16}O$	0.152 ± 0.088	0.744 ± 0.314	0.381 ± 0.174

Note: * indicates compounds appear in 3 flowering periods of *Magnolia grandiflora*. # indicates compounds appear in the specific flowering period; - indicates the compound was not detected in that flowering period.

References

1. Pichersky, E.; Noel, J.P.; Dudareva, N. Biosynthesis of plant volatiles: Nature's diversity and ingenuity. *Science* **2006**, *311*, 808–811. [PubMed]
2. Baldwin, I.T. Plant volatiles. *Curr. Biol.* **2010**, *20*, 392–397. [CrossRef]
3. Bottalico, F.; Chirici, G.; Giannetti, F.; De Marco, A.; Nocentini, S.; Paoletti, E.; Travaglini, D. Air pollution removal by green infrastructures and urban forests in the city of Florence. *Agric. Agric. Sci. Procedia* **2016**, *8*, 243–251. [CrossRef]
4. Li, Q.; Kobayashi, M.; Kumeda, S.; Ochiai, T.; Miura, T.; Kagawa, T.; Kawada, T. Effects of Forest Bathing on Cardiovascular and Metabolic Parameters in Middle-Aged Males. *Evid.-Based Complement. Altern. Med.* **2016**, *2016*, 2587381.
5. Lebanov, L.; Tedone, L.; Kaykhaii, M. Multidimensional Gas Chromatography in *Essential oil* Analysis. Part 2: Application to Characterisation and Identification. *Chromatographia* **2019**, *82*, 399–414. [CrossRef]
6. Lv, Y.; Zhang, J.N.; Zhao, J. Analysis of Volatile Compounds in the Flowers of *Elaeagnus angustifolia* L. by Automatic GC-MS Data Analysis Strategy. *Chem. Reagents* **2022**, *4*, 1657–1664. [CrossRef]
7. Yuan, J.L.; Jin, X.L.; Zhang, Z. Volatility Compounds of *Michelia crassipes* Tepals at Different Flowering Stages. *Acta Hortic. Sin.* **2023**, *50*, 1095–1109. [CrossRef]
8. Yang, Y.; Yan, S.; Chen, Q. Volatile Compounds from flowers at different periods and from floral organs at full flowering period of *Rosa banksiae* Ait. var. Banksiae. *J. Northwest A&F Univ.* **2025**, *53*, 110–121. [CrossRef]
9. Yang, M.; Li, Q.Y.; Xiang, Z.L. Comparative analysis of aroma volatiles in different flowering stages and organs of *Camellia handelii* and *Camellia uraku* (Mak.) Kitamura. *J. Cent. China Norm. Univ.* **2023**, *57*, 539–547+560. [CrossRef]
10. Cheng, T.Y.; Ma, K.; Fan, X.Z. Analysis on volatile Compounds of various parts of chicory from Guizhou using HS-HPME-GC-MS. *China Food Addit.* **2024**, *35*, 188–199. [CrossRef]
11. Zhu, J.C.; Liu, X.J.; Niu, Y.W. Analysis of characteristic aroma compounds in Longjing tea based on 2-dimensional gas chromatography-mass spectrometr. *China Food Addit.* **2024**, *35*, 229–237. [CrossRef]
12. Liu, X.J.; Kan, M.; Zhang, W.Y. Identification of Volatile Characteristic Aroma Compounds of Abies Densa Griff by Gas Chromatography-Mass Spectrometry-Olfactory. *Flavour Frag. Cosmet.* **2025**, *4*, 1–5. [CrossRef]
13. Xiong, Q.Q.; Fan, J.J.; Ma, J.Z. Establishment of determination method of cherry blossom fragrance based on electronic nose technology. *Non-Wood For. Res.* **2024**, *42*, 281–288. [CrossRef]
14. Zhu, K.Y.; Yang, R.Q.; Zhao, Y.Y. Odor Differences of Aucklandiae Radix from Different Origins Based on Electronic Nose and HS-GC-MS. *Mod. Chin. Med.* **2025**, *27*, 638–646. [CrossRef]
15. Ji-Won, A.; Trieu-Vuong, D.; Shin-Young, P. Characteristics of biogenic volatile organic compounds emitted from major species of street trees and urban forests. *Atmos. Pollut. Res.* **2022**, *13*, 101470.
16. Niu, Y.; Yan, Y.; Chai, J. Effects of regional transport from different potential pollution areas on volatile organic compounds (VOCs) in Northern Beijing during non-heating and heating periods. *Sci. Total Environ.* **2022**, *836*, 155465. [CrossRef]
17. Sindhu, S.; Jain, C.D.; Ratnam, M.V. Understanding the effect of seasonal variability of VOCs and NOx on the ozone budget and its photochemical processing over a rural atmosphere. *Environ. Sci. Pollut. Res.* **2025**, *32*, 6770–6783. [CrossRef] [PubMed]
18. Nuvolone, D.; Petri, D.; Voller, F. The effects of ozone on human health. *Environ. Sci. Pollut. Res.* **2018**, *25*, 8074–8088.
19. Kinney, P.L. Interactions of Climate Change, Air Pollution, and Human Health. *Curr. Environ. Health Rep.* **2018**, *5*, 179–186. [CrossRef]
20. Zhang, Q.; Xue, Z.; Yi, L.; Wang, J.; Liu, E. Temperature Regulates BVOCs-Induced O_3 Formation Potential Across Various Vegetation Types in the Sichuan Basin, China. *Forests* **2025**, *16*, 1091. [CrossRef]
21. Yenisoy-Karakaş, S.; Dörter, M.; Odabasi, M. Intraday and interday variations of 69 volatile organic compounds (BVOCs and AVOCs) and their source profiles at a semi-urban site. *Sci. Total Environ.* **2020**, *723*, 138028. [PubMed]
22. Carter, W.P.L. *Updated Maximum Incremental Reactivity Scale and Hydrocarbon Bin Reactivities for Regulatory Applications*; California Air Resources Board: Sacramento, CA, USA, 2009. Available online: https://ww2.arb.ca.gov/sites/default/files/barcu/regact/2009/mir2009/mir10.pdf (accessed on 1 December 2025).
23. Kirchner, F.; Jeanneret, F.; Clappier, A. Total VOC reactivity in the planetary boundary layer: 2. A new indicator for determining the sensitivity of the O_3 production to VOC and NOx. *J. Geophys. Res.-Atmos.* **2001**, *106*, 3095–3110. [CrossRef]
24. Kumar, V.; Sinha, V. Season-wise analyses of VOCs, hydroxyl radicals and O_3 formation chemistry over north-west India reveal isoprene and acetaldehyde as the most potent O_3 precursors throughout the year. *Chemosphere* **2021**, *283*, 131184. [CrossRef] [PubMed]
25. Alvim, D.S.; Gatti, L.V.; Corrêa, S.M. Determining VOCs Reactivity for O_3 Forming Potential in the Megacity of São Paulo. *Aerosol Air Qual. Res.* **2018**, *18*, 2460–2474. [CrossRef]
26. Jain, C.D.; Ratnam, M.V.; Madhavan, B.L. Impact of regional transport on total OX (NO_2 + O_3) concentrations observed at a tropical rural location. *Atmos. Pollut. Res.* **2022**, *13*, 101408. [CrossRef]
27. Baghi, R.; Helmig, D.; Guenther, A.; Duhl, T. Contribution of flowering trees to urban atmospheric biogenic volatile organic compound emissions. *Biogeosciences* **2012**, *9*, 3777–3785. [CrossRef]

28. Eisenman, T.S.; Churkina, G.; Jariwala, S.P. Urban trees, air quality, and asthma: An interdisciplinary review. *Landsc. Urban Plan.* **2019**, *187*, 47–59. [CrossRef]
29. Unger, N. Human land-use-driven reduction of forest volatiles cools global climate. *Nat. Clim. Change* **2014**, *4*, 907–910.
30. Wu, J.; Long, J.; Liu, H. Biogenic volatile organic compounds from 14 landscape woody species: Tree species selection in the construction of urban greenspace with forest healthcare effects. *J. Environ. Manag.* **2021**, *300*, 113761. [CrossRef]
31. Wei, X.Y.; Zhang, Y.N.; Bai, L.L. GC-MS Analysis and Antibacterial Activity Study of Paulownia Flower Oil. *Nat. Prod. Res. Dev.* **2008**, *1*, 87–90. [CrossRef]
32. Ding, F.W.; Peng, Y.L.; Li, M. Analysis on Volatile Oil of *Melia azedarach* Flowers by GC/M S. *Food Drug* **2010**, *12*, 99–102.
33. Cai, G.X.; Liu, Y.X.; Hu, W.B. Study on Chemical Constituents and Antioxidant Activity of the *Essential oil* of Flowers of *Magnolia grandiflora* L. *Chem. Bioeng.* **2012**, *29*, 91–94.
34. Feng, Y.Z.; Yang, C.W.; Wang, B.P. Determination of volatile Compounds in the flowers of different Paulownia species based on HS-SPME and GC-MS. *Nat. Prod. Res. Dev.* **2023**, *35*, 1163–1171.
35. Gao, M.; Yan, C.; Li, N. Electrosmotic coupled with particle-assisted deep eutectic solvent flotation for the enrichment of eugenol from clove. *Microchem. J.* **2024**, *205*, 111326. [CrossRef]
36. Xia, S.Q.; Wang, P.L.; Chen, S.Y. Stability of Citral Sustained-release Preparation and Its Inhibitory Effect on *Aspergillus flavus*. *Sci. Technol. Food Ind.* **2022**, *43*, 85–92.
37. Pang, Y.R.; Hu, Z.H.; Xiao, D.G. Advances in metabolic engineering for the microbial production of naturally occurring terpenes-limonene and bisabolene: A mini review. *Chin. J. Biotechnol.* **2018**, *34*, 24–33. [CrossRef]
38. Wen, K.; Yang, G.E.; Yang, H.Z. Study on optimized synthesis process of geranylacetone from linalool by response surface method. *Appl. Chem. Ind.* **2023**, *52*, 1414–1419. [CrossRef]
39. Zhao, Z.D.; Su, W.Q.; Chen, F.Y. Research Progress on the Resources and Bioactive Applications of Acacia Alcohol. *Chem. Ind. For. Prod.* **2005**, *S1*, 175–178.
40. Xiong, C.; Li, Q.; Li, S. In vitro antimicrobial activities and mechanism of 1-octen-3-ol against food-related bacteria and pathogenic fungi. *J. Oleo Sci.* **2017**, *66*, 1041–1049.
41. Zhang, W.; Cheng, Z.H.; Liu, Y.G. The bactericidal and aromatic substance of volatile gas of the plant. *Ecol. Environ. Sci.* **2007**, *5*, 1455–1459. [CrossRef]
42. Cai, H.Q.; Tian, H.J.; Huang, H. Inhibition effect of four plant essential oils on nine aquatic pathogens. *Feed Res.* **2025**, *48*, 66–72. [CrossRef]
43. Li, X.; Xia, M.; Hu, C. The regulation on molecular properties of trans-cinnamaldehyde (trans-3-phenylprop-2-enaldehyde) by external physical electric field. *Results Chem.* **2025**, *16*, 102376. [CrossRef]
44. Zhe, H.Y.; Yang, S.M.; Shang, Z.W. Evaluation of the Antibacterial Effect of two Perilla *Essential oil* in Vitro. *J. Mt. Agric. Biol.* **2021**, *40*, 34–39. [CrossRef]
45. Zhu, L.; Lu, X.X.; Xue, N.N. Compounds Analysis and in vitro Activity of Essential Oils from *Cedrus atlantica*. *Food Res. Dev.* **2023**, *44*, 151–156+184.
46. Wei, T.; Regeard, C.; Barroca-Aubry, N. Chemoenzymatic oxidation of citronellol and geraniol: Synthesis and antibacterial activity assessment. *Colloids Surf. B Biointerfaces* **2025**, *253*, 114723. [CrossRef]
47. Wang, P.; Zhang, H.Y.; Liu, Y.M. Research progress on chemical constituents, pharmacological effects and clinical application of volatile oil from *Magnolia liliflora*. *China Pharm.* **2022**, *33*, 378–384.
48. Mehmood, T.; Afzal, A.; Anwar, F. Variations in the composition, antibacterial and haemolytic activities of peel essential oils from unripe and ripened *Citrus limon* (L.) Osbeck fruit. *J. Essent. Oil Bear Plants* **2019**, *22*, 159–168.
49. Krist, S.; Halwachs, L.; Sallaberger, G. Effects of scents on airborne microbes, part I: Thymol, eugenol, trans -cinnamaldehyde and linalool. *Flavour Fragr. J.* **2007**, *22*, 44–48. [CrossRef]
50. Kei, S.; Sabine, K.; Gerhard, B. Antimicrobial effect of trans-cinnamaldehyde, (-)-perillaldehyde, (-)-citronellal, citral, eugenol and carvacrol on airborne microbes using an airwasher. *Biol. Pharm. Bull.* **2006**, *29*, 2292–2294. [CrossRef]
51. Bao, X.E.; Bao, H.; Zhao, L.L. Volatile organic compound emission characteristics of crops on the Inner Mongolia Plateau. *J. Ecol. Environ.* **2025**, *34*, 1442. [CrossRef]
52. Wu, K.; Yang, X.; Chen, D. Estimation of biogenic VOC emissions and their corresponding impact on ozone and secondary organic aerosol formation in China. *Atmos. Res.* **2020**, *231*, 104656. [CrossRef]
53. Chang, J.; Ren, Y.; Shi, Y. An inventory of biogenic volatile organic compounds for a subtropical urban–rural complex. *Atmos. Environ.* **2012**, *56*, 115–123. [CrossRef]
54. Guo, X.Y. Analysis of volatile compositions in 6 edible fragrant plants by GC-MS/GC-O technology. *Trans. Chin. Soc. Agric. Eng.* **2019**, *35*, 299–307.
55. Xiong, H.P.; He, G.Q.; Yuan, C.G. Advancement of Studying on Leaf Alcohol. *China Food Addit.* **2004**, *6*, 34–37+45.
56. Song, S.Q.; Gu, M.; Chen, F.P. Analysis of Volatile Compounds in Flowers and Leaves of *Thymus mongolicus* with Solid Phase Microextraction by GC/MS. *Subtrop. Plant Sci.* **2017**, *46*, 244.

57. Nazarinia, D.; Moslehi, A.; Hashemi, P. (-)-α-bisabolol exerts neuroprotective effects against pentylenetetrazole-induced seizures in rats by targeting inflammation and oxidative stress. *Physiol. Behav.* **2023**, *272*, 114351. [CrossRef]
58. Yang, T.; Li, D.D.; Shan, X.L. Pollution characterization, source apportionment and health risk assessment of Benzene Homologues in the ambient air of a typical urban area in Beijing, China. *Asian J. Ecotoxicol.* **2017**, *12*, 79–97.
59. Liao, S.; Zhang, J.; Shi, S. Association of aldehyde exposure with cardiovascular disease. *Ecotoxicol. Environ. Safe* **2020**, *206*, 111385.
60. McCloskey, S.E.; Gershanik, J.J.; Lertora, J.J.L. Toxicity of benzyl alcohol in adult and neonatal mice. *J. Pharm. Sci.* **1986**, *75*, 702–705. [CrossRef]

Disclaimer/Publisher's Note: The statements, opinions and data contained in all publications are solely those of the individual author(s) and contributor(s) and not of MDPI and/or the editor(s). MDPI and/or the editor(s) disclaim responsibility for any injury to people or property resulting from any ideas, methods, instructions or products referred to in the content.